Ore Geology Reviews 75 (2016) 42–51

Contents lists available at ScienceDirect

Ore Geology Reviews

journal homepage: www.elsevier.com/locate/oregeorev

Risk quantification with combined use of lithological and grade simulations: Application to a porphyry copper deposit

Hassan Talebi [a,b], Elham Hosseinzadeh Sabeti [a], Mehdi Azadi [a], Xavier Emery [c,d]

[a] Department of Mining Engineering, University of Tehran, Iran
[b] Faculty of Health, Engineering and Science, Edith Cowan University, Perth, Australia
[c] Department of Mining Engineering, University of Chile, Santiago, Chile
[d] Advanced Mining Technology Center, University of Chile, Santiago, Chile

ARTICLE INFO

Article history:
Received 21 May 2015
Received in revised form 15 November 2015
Accepted 11 December 2015
Available online 14 December 2015

Keywords:
Uncertainty modeling
Plurigaussian model
Geostatistics
Geological control

ABSTRACT

The uncertainty in the recoverable tonnages and grades in a mineral deposit is a key factor in the decision-making process of a mining project. Currently, the most prevalent approach to model the uncertainty in the spatial distribution of mineral grades is to divide the deposit into domains based on geological interpretation and to predict the grades within each domain separately. This approach defines just one interpretation of the geological domain layout and does not offer any measure of the uncertainty in the position of the domain boundaries and in the mineral grades. This uncertainty can be evaluated by use of geostatistical simulation methods. The aim of this study is to evaluate how the simulation of rock type domains and grades affects the resources model of Sungun porphyry copper deposit, northwestern Iran. Specifically, three main rock type domains (porphyry, skarn and late-injected dykes) that control the copper grade distribution are simulated over the region of interest using the plurigaussian model. The copper grades are then simulated in cascade, generating one grade realization for each rock type realization. The simulated grades are finally compared to those obtained using traditional approaches against production data.

1. Introduction

Currently, the most common approach to model the uncertainty in the spatial distribution of mineral grades in an ore deposit is to define geological domains deterministically, then to predict or to simulate the mineral grades within each domain conditionally to the data belonging to this domain. This approach consists in interpreting the geological domains, using experimental data of lithology, mineralogy and/or alteration and geological knowledge of the deposit (Dowd, 1986; Duke and Hanna, 2001; Sinclair and Blackwell, 2002; Rossi and Deutsch, 2014). However, it suggests only one interpretation of the geological domains and fails at measuring the uncertainty in the spatial configuration of these domains. By constructing multiple numerical outcomes or realizations of the geological domains, geostatistical simulation helps to improve the geological interpretation and to measure the uncertainty in the position of the domain boundaries. This ability of geostatistical simulation allows assessing, in a realistic way, the risk of a mining project by considering the uncertainty in both the geological interpretation and the grade distribution. Several methods can be used to this end, including sequential indicator (Journel and Alabert, 1990; Journel and Gómez-Hernández, 1993; Deutsch, 2006), multiple-point (Strebelle, 2002; Mariethoz and Caers, 2015), truncated Gaussian (Matheron et al., 1987; Galli et al., 1994) and plurigaussian (Galli et al., 1994; Le Loc'h et al., 1994; Armstrong et al., 2011) simulation. In particular, plurigaussian simulation has gained popularity and proved to be versatile to reproduce complex configurations of geological domains (Riquelme et al., 2008; Yunsel and Ersoy, 2013; Talebi et al., 2013, 2014; Rezaee et al., 2014; Madani and Emery, 2015).

The aim of this study is to investigate the impact of simulated models instead of deterministic geological models for studying the risk in the evaluation of mineral resources and ore reserves, through a case study on the Sungun copper deposit, located in northwestern Iran. This deposit has been identified both as a skarn and a porphyry-type deposit. It is characterized by the presence of late-injected dykes with variable density, size and geometry into the main intrusion mass of the deposit. These dykes often do not have any mineralization and consequently dilute the mill feed (Hezarkhani and Williams-Jones, 1998), while porphyry and skarn correspond to ore with different grade distributions and structures. In this type of deposits, the risk due to uncertainty of geological contacts is essential. First of all, the plurigaussian model is applied to the three main rock types (porphyry, skarn and late-injected dykes) in order to reproduce the spatial variability of the rock type domains and to assess the uncertainty in the position of their boundaries. One hundred realizations (outcomes) are generated and, afterwards, each of these is used to further generate a copper grade

E-mail addresses: h.talebi@ut.ac.ir (H. Talebi), e.hosseinzadeh@ut.ac.ir (E.H. Sabeti), mehdiazadi@ut.ac.ir (M. Azadi), xemery@ing.uchile.cl (X. Emery).

http://dx.doi.org/10.1016/j.oregeorev.2015.12.007
0169-1368/

realization constructed with the sequential Gaussian simulation (Goovaerts, 1997). The realizations are then used to quantify uncertainty in recoverable tonnage and grade. The results are compared against traditional approaches and against production data.

2. Methodology

2.1. Principles of geostatistical simulation

An ore deposit can be characterized by one or more regionalized variables, i.e., variables that are distributed in space and exhibit some continuity, such as the grades of elements of economic interest or of contaminants, the rock type or the alteration intensity, to name a few examples. The exact values of these variables are known at a finite set of sampling locations, but unknown elsewhere. In order to quantify the uncertainty in the values at unsampled locations, one assumes that each regionalized variable is a realization of a spatial random field, characterized by its finite-dimensional distributions (Chilès and Delfiner, 2012). Once the random field model is specified, it is possible to draw different realizations or outcomes of this field and to constrain these realizations to reproduce the known values at sampling locations (conditional simulation). A variety of random field models and simulation algorithms have been developed in the past decades; the reader is referred to the textbooks by Lantuéjoul (2002) or Chilès and Delfiner (2012) for an overview.

2.2. Sequential simulation of grades

Let us denote by $z(\mathbf{x})$ the grade of an element of interest at a specific location $\mathbf{x}$ in the deposit, and by D the domain in which the grade is studied. The regionalized variable $\{z(\mathbf{x}): \mathbf{x} \in D\}$ is viewed as a realization of a parent random field $\{Z(\mathbf{x}): \mathbf{x} \in D\}$. Commonly, this random field is modeled as a monotonic transformation of a stationary standard Gaussian random field $\{Y(\mathbf{x}): \mathbf{x} \in D\}$, which implies that the grade data have to be transformed into normally-distributed data prior to simulation and that, after simulation, the realizations have to be back-transformed into grades, a procedure known as anamorphosis (Chilès and Delfiner, 2012). A stationary Gaussian random field is characterized by its mean value, constant over space, and by its auto-covariance function or its variogram.

The simulation of the Gaussian random field at a set of target locations can be performed through the following steps (Goovaerts, 1997; Deutsch and Journel, 1998; Remy et al., 2009):

1. Obtain a representative histogram for the input data.
2. Transform the data into normal scores (anamorphosis).
3. Calculate the sample variogram of the normal scores data and fit a variogram model.
4. Select a target location for which the value has not been yet simulated.
5. Perform simple kriging at the target location, using the input normal scores data and the already simulated values. Obtain a prediction and a variance of the prediction error.
6. Draw a random value from a Gaussian distribution with mean equal to the simple kriging prediction and variance equal to the simple kriging variance.
7. Incorporate the value drawn into the conditioning data set.
8. Repeat steps 4–7 until all the target locations are visited.
9. Back-transform the simulated Gaussian values into the original grade scale.
10. Repeat steps 4–9 to generate another realization.

2.3. Plurigaussian simulation of geological domains

Let now $z(\mathbf{x})$ denote the value of a geological domain (codified as, say, an integer between 1 and n) at location $\mathbf{x}$. In the plurigaussian model, this value is interpreted as a realization of an integer random field $\{I(\mathbf{x}): \mathbf{x} \in D\}$ obtained by truncating one or several underlying Gaussian random fields, according to a given truncation rule.

Specifically, consider a set of m stationary Gaussian random fields $\{Y_i(\mathbf{x}): \mathbf{x} \in D\}$ with $i = 1 \ldots m$, which can be viewed as the components of a vector Gaussian random field $\{\boldsymbol{Y}(\mathbf{x}): \mathbf{x} \in D\}$. Also consider a partition of R^m into n disjoint subdomains $D_1, \ldots, D_n$ and define an integer random field by.

$$\forall \mathbf{x} \in D, I(\mathbf{x}) = i \text{ if and only if } \boldsymbol{Y}(\mathbf{x}) \in D_i. \quad (1)$$

The geometry of the partition $(D_1, \ldots, D_n)$ defines the so-called truncation rule, which controls the spatial relationships between the geological domains. Usually, the subdomains forming the partition are cuboids of R^m (Emery, 2007; Armstrong et al., 2011). The specific values that define the boundaries of such cuboids are known as the truncation thresholds and are related to the proportion of space covered by each geological domain.

As an example, consider two independent Gaussian random fields (Y_1 and Y_2) and the following truncation rule to define the domain at location $\mathbf{x}$:

$$I(\mathbf{x}) = \begin{cases} 1 & \text{if } Y_1(\mathbf{x}) < t_1 \\ 2 & \text{if } Y_1(\mathbf{x}) \geq t_1 \text{ and } Y_2(\mathbf{x}) < t_2 \\ 3 & \text{if } Y_1(\mathbf{x}) \geq t_1 \text{ and } Y_2(\mathbf{x}) \geq t_2 \end{cases} \quad (2)$$

where t_1 and t_2 are the threshold values. Geometrically, this truncation rule can be represented by a two-dimensional flag, where each axis represents a Gaussian random field and the rectangular areas correspond to the couples of Gaussian values associated with each domain (Fig. 1). The choice of the truncation rule may be based on topological or chronological relationships between geological domains. For instance, domain 1 may correspond to a younger domain that crosscuts the other two domains (Madani and Emery, 2015). The values of thresholds t_1 and t_2 determine the proportion of space covered by each domain. For example, if they are equal to zero (median of the standard Gaussian distribution), then the Gaussian random fields take values below the thresholds half of the time and values above the thresholds half of the time, which means that domain 1 will have a proportion of 0.5, while the proportions of domains 2 and 3 will be 0.25.

To complete the specification of the model, one has to infer the correlation structure of the vector Gaussian random field $\{\boldsymbol{Y}(\mathbf{x}): \mathbf{x} \in D\}$. This is done in order to fit the correlation structure of the integer random field $\{I(\mathbf{x}): \mathbf{x} \in D\}$, which is experimentally known from the available data on the geological domains prevailing at the sampling locations (Armstrong et al., 2011).

The steps for simulation are the following:

1. Define the truncation rule.
2. Define the truncation thresholds.
3. Define the correlation structure of the underlying Gaussian random fields, via its impact on the indicator variograms of the integer field $I(\mathbf{x})$.
4. At the sampling locations, transform the integer data into Gaussian data. This can be done with an iterative method known as Gibbs sampler (Lantuéjoul, 2002).
5. Simulate the Gaussian random fields at the target locations, conditionally to their values at the sampling locations. This can be done with the sequential algorithm described in the previous section.
6. Truncate the simulated Gaussian random fields to obtain an integer random field.
7. Repeat steps 4–6 to generate another realization.

2.4. Cascade simulation of geological domains and grades

The cascade approach consists in simulating first the layout of the geological domains, then the mineral grades within each domain

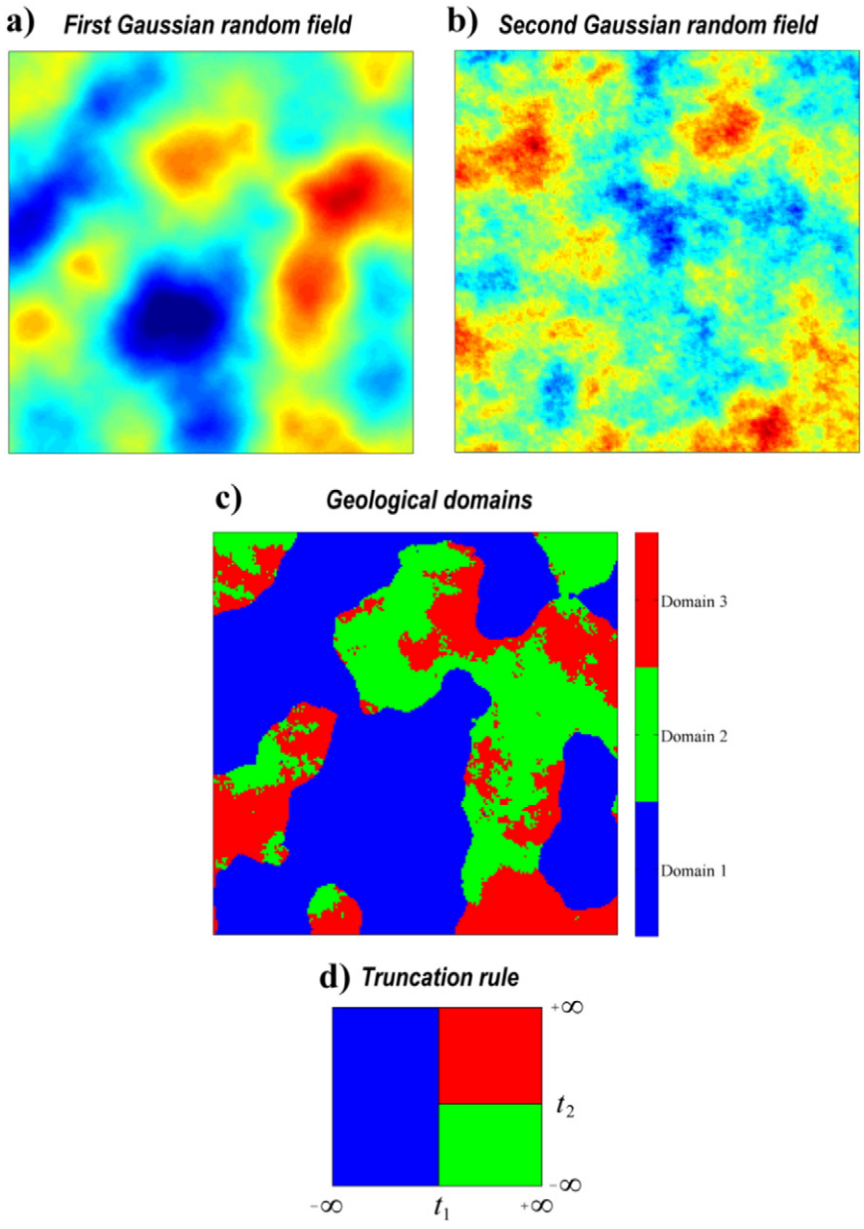

Fig. 1. Realizations of two Gaussian random fields (a, b) and of three domains (c) obtained by applying the truncation rule (d).

conditionally to the grade data belonging to this domain only (Chilès and Delfiner, 2012; Roldão et al., 2012). The steps are the following:

1. Simulate the geological domains using plurigaussian simulation (Section 2.3).
2. Select the conditioning data located in domain 1 and the target locations that have been simulated as domain 1.
3. Simulate the grade at these target locations using sequential simulation (Section 2.2).
4. Repeat steps 2–3 to simulate the grade in the other domains.
5. Repeat steps 1–4 to generate another realization.

3. Case study: Sungun copper deposit

3.1. Geological description

The Sungun porphyry copper deposit is located in northwestern Iran, on the well-known Urmia-Dokhtar Magmatic Arc (UDMA, Fig. 2). Most of the Iranian porphyry copper deposits were formed during the magmatic activities of this arc (Shahabpour, 2005; Hezarkhani, 2006b; Shahabpour, 2007; Boomeri et al., 2010; Dargahi et al., 2010; Shafiei, 2010; Hou et al., 2011; Afshooni et al., 2013; Azadi et al., 2015). The remains of ancient tunnels and smelting furnaces in the area of interest show that copper ores used to be exploited in the skarn zone, and were the center of attention before the discovery of the porphyry copper deposit by Etminan (1977) in the adjacent stock (Calagari and Hosseinzadeh, 2006). The oldest rocks exposed in the study area are a 500 m sequence of Cretaceous limestone with intercalations of shale, and a 1500 m thick sequence of Middle to early Late Tertiary, intermediate, calc-alkaline lavas, and tuffaceous rocks, intruded by numerous calc-alkaline andesitic dykes (Hezarkhani, 2006a; Fig. 2). The deposit is associated with diorite–granodiorite to quartz monzonite of Miocene age that intruded Eocene volcano-sedimentary and Cretaceous carbonate rocks. Several intrusive pulses are observable in the emplacement of the Sungun stock and also hydrothermal activities that are associated with this mineralization (Hezarkhani and Williams-Jones, 1998; Hezarkhani, 2006a; Fig. 2). Skarn-type alteration and associated mineralization occurs as a rim along the eastern and northern margins of the

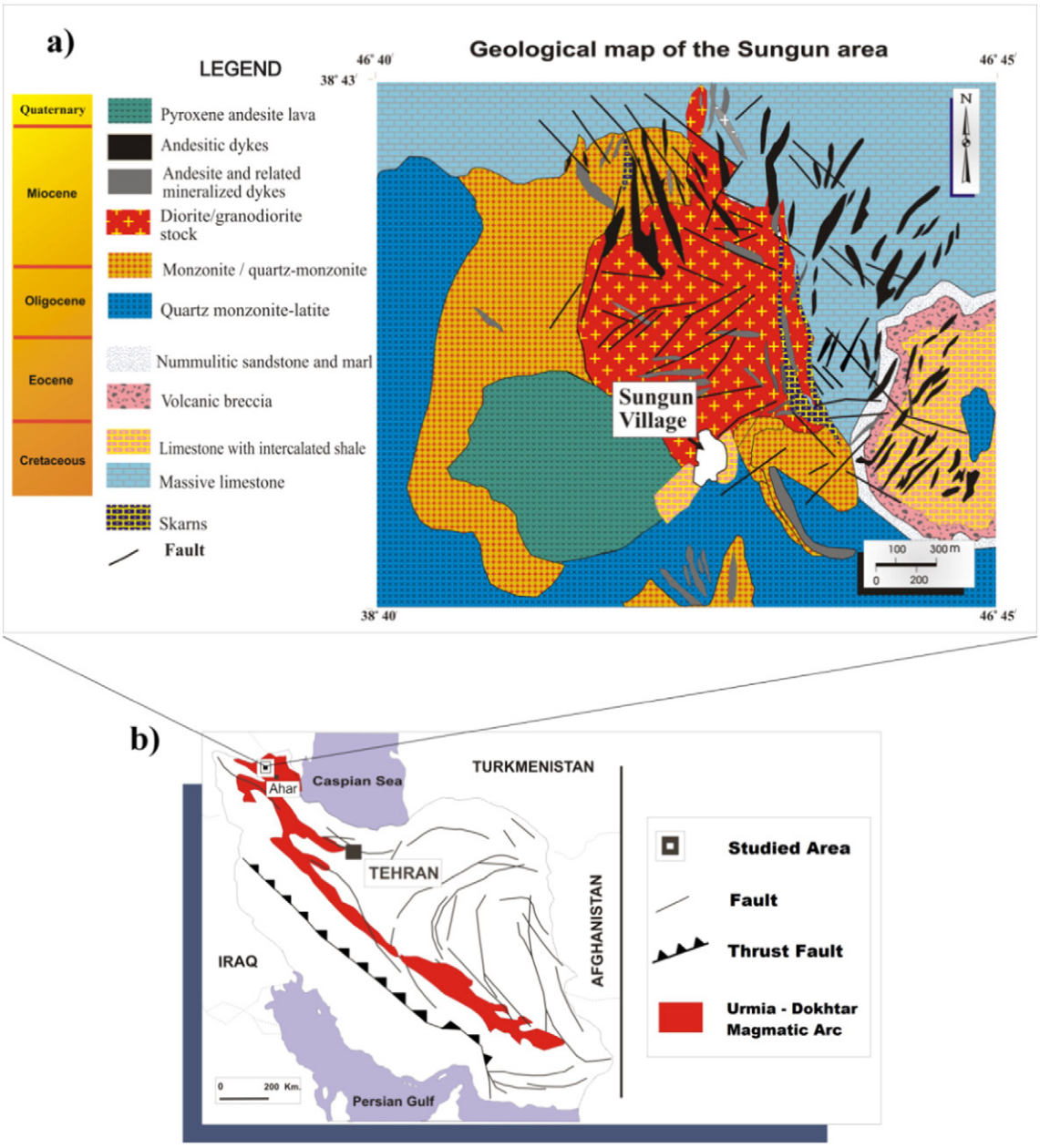

Fig. 2. a) Geological map of Sungun showing different rock domains (Hezarkhani, 2006a); and b) map of Iran showing Urmia-Dokhtar Magmatic Arc (UDMA).

stock (Lescuyer et al., 1978; Mehrpartou, 1993). Late-injected dykes are distributed mostly in the north and eastern parts of the Sungun deposit (outside the main stock, Fig. 2). Most of these dykes rarely have mineralization or are poorly mineralized (0.08% copper in average), and their thicknesses vary from a few centimeters to several tens of meters (Hezarkhani, 2006a).

Previous studies on the geological features of this deposit revealed three main rock type domains controlling the copper grade distribution (Hezarkhani and Williams-Jones, 1998; Calagari and Hosseinzadeh, 2006; Calagari, 2003, 2004; Hezarkhani, 2006a; Asghari et al., 2009): Sungun porphyry (SP) stock, skarn mineralization (SK), and late-injected dykes (DK). These domains are discussed in detail in the next subsections.

3.1.1. Sungun porphyry (SP) stock

The multiphase porphyry stock at Sungun is composed of monzonite/quartz monzonite and diorite/granodiorite in order of emplacement (Fig. 2). The monzonite/quartz-monzonites are mainly porphyritic, and exposed to the west of the diorite/granodiorite intrusion, and in a small body in the southeast. The diorite/granodiorite forms the central part of the stock and intrudes the monzonite/quartz-monzonite (Hezarkhani, 2006a). Potassic and phyllic hydrothermal alteration and the mineralization at Sungun are centered on the diorite/granodiorite intrusion and were broadly synchronous with its emplacement (Hezarkhani, 2002; Fig. 2). According to Hezarkhani and Williams-Jones (1998), early hydrothermal alteration was dominantly potassic, and was followed by later phyllic alteration. The earliest alteration in diorite/granodiorite, which was produced by fluxes of magmatic fluids away from the pluton center, is represented by potassic mineral assemblages developed pervasively and as halos around veins in the deep and central parts of the Sungun stock. The change from potassic alteration to phyllic alteration is transitional. Influx of meteoric water into the central part of the system and mixing with magmatic fluid produced phyllic alteration that is characterized by the replacement of almost all rock-forming silicates by sericite and quartz, and overprints the earlier formed potassic zone (Hezarkhani and Williams-Jones, 1998).

Table 1
Statistics of copper grade (%), in the overall deposit and for each rock type domain.

	Number of data	Mean	Median	Std. deviation	Variance	Minimum	Maximum
DK	9016	0.08	0.01	0.22	0.05	0	3.58
SK	749	0.57	0.26	1.28	1.64	0	23.50
SP	20,664	0.54	0.46	0.48	0.23	0	9.61
Total	30,429	0.40	0.25	0.51	0.26	0	23.50

Hypogene mineralization occurs as disseminations, fracture and microfracture fillings. Pyrite is the most abundant sulfide, and chalcopyrite is the dominant copper ore, accompanied by minor amounts of molybdenite and trace amounts of bornite, tetrahedrite, and hypogene chalcocite (Calagari, 2004).

3.1.2. Skarn mineralization (SK)

The contact between granodioritic rocks and Cretaceous limestone is well exposed in the northern and eastern parts of the study area (Fig. 2). Intrusion of granodioritic rocks into the limestone has altered it to skarn that locally contains abundant copper mineralization (Hezarkhani, 2006a). Based on Calagari and Hosseinzadeh (2006), the skarnification process occurred in two stages: prograde and retrograde. During the prograde stage, considerable amounts of medium- to coarse-grained anhydrous calc-silicates formed. In the retrograde stage, the previously formed skarn assemblages were affected by intense multiple hydro-fracturing phases in the copper-bearing stock. Consequently, considerable amounts of hydrous calc-silicates (epidote, tremolite–actinolite), sulfides (pyrite, chalcopyrite, galena, sphalerite, bornite), oxides (magnetite, hematite) and carbonates (calcite, ankerite) replaced the anhydrous calc-silicates (Calagari and Hosseinzadeh, 2006). The associated contact metasomatic alteration and mineralization are best developed in places where the fracture density in the carbonate rocks is relatively high. The abundance and type of opaques vary spatially, depending on the locality and distance from the intrusive contact. Sulfides are predominantly present in the skarn zone and their abundance is almost restricted to within 0–20 m from the contact; further away their abundance sharply diminishes (Calagari and Hosseinzadeh, 2006).

3.1.3. Late-injected dykes (DK)

Two types of dykes have been injected into the igneous rocks with abrupt contacts: (1) light-brown altered and mineralized andesitic dykes; and (2) dark-brown, almost fresh, un-mineralized (post-mineralization) andesitic dykes (Hezarkhani and Williams-Jones, 1998; Calagari, 2003; Hezarkhani, 2006a). Both types crosscut older rocks and their thicknesses vary from a few centimeters to several tens of meters. The thicknesses vary vertically and horizontally, even in a single dyke, and none of the dykes is flatly planar. In fact, most of them are curved and do not follow a single direction. The area has suffered from multiple structural activities and some of the four main fault systems have dislocated the dykes.

On the one hand, mineralized dykes are dominant in diorite/granodiorite rocks in the center of the stock (the area of interest in this study; Calagari, 2003) and are pervasively affected by phyllic alterations, with a poor mineralization. These rocks are of early dykes and are thought to be injected almost nearly after the main stock (Hezarkhani, 2006a, 2006b). Mineralization in these rocks is more limited to the margins of the dykes, in contact with the highly altered intrusive rocks. The mineralization in these dykes is believed to be introduced during the influx of meteoric water into the central part of the system and mixing with magmatic fluid and formation of phyllic alteration (Hezarkhani and Williams-Jones, 1998). On the other hand, un-mineralized late dykes, which crosscut monzonite/quartz-monzonite in the north, are fresh, unaltered rocks with no mineralization (Hezarkhani, 2006a). From the mining point of view, either the dykes bear a weak mineralization or no mineralization, are all considered as waste, insofar as the average copper grade in Sungun dykes is 0.08%, with a variance of 0.05 (Table 1).

3.2. Presentation of the data set

A set of 34,037 diamond drill hole samples, located in a volume of 1200 m × 1100 m × 1000 m (Fig. 3), is available with information on the rock types (SP, SK or DK) and, for 30,429 of these samples, on the total copper grades. A summary of descriptive statistics is given in Table 1, globally and per rock type domain, while Fig. 4 shows the grade distributions via box plots and histograms. From this table and figure, one observes that the distributions of copper grade strongly differ with the rock type, suggesting that the data are a mixture of different populations. On the one hand, SP and SK have a high average grade, but the grade variability is quite different between these two domains. On the other hand, DK has almost no economic mineralization and corresponds to waste material not to be sent to the processing plant. These facts force mine geologists to separate the rock type domains prior to the resources evaluation process, since different grade distributions are expected in these domains.

3.3. Plurigaussian simulation of rock type domains

As the rock type domains are mutually in contact, two independent Gaussian random fields $\{Y_1, Y_2\}$ and two thresholds $\{t_1, t_2\}$ are used with the same truncation rule as in Fig. 1. The second random field (Y_2) is applied to separate the two oldest domains (SK = code 2 and SP = code 3), which have a roughly similar anisotropy and irregular boundary, while the first random field (Y_1) is used to erode these two domains by the late-injected dykes (DK = code 1) that have a lower average copper grade. These dykes have more regular boundaries than the other

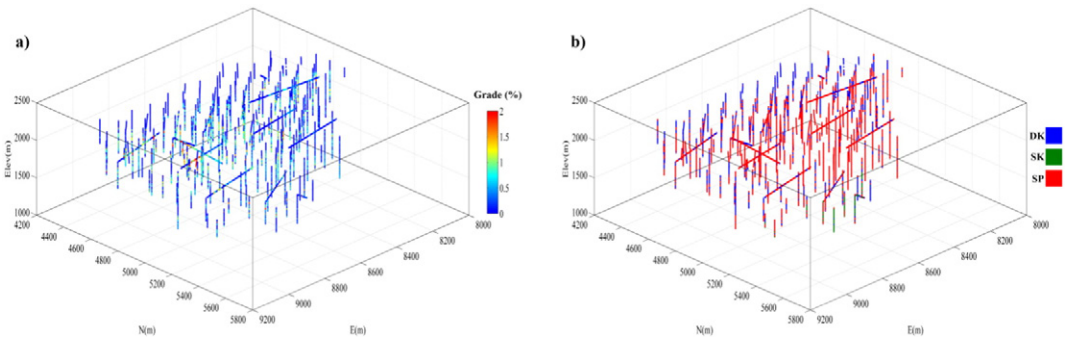

Fig. 3. Perspective view of available drill hole samples showing a) copper grade and b) rock type.

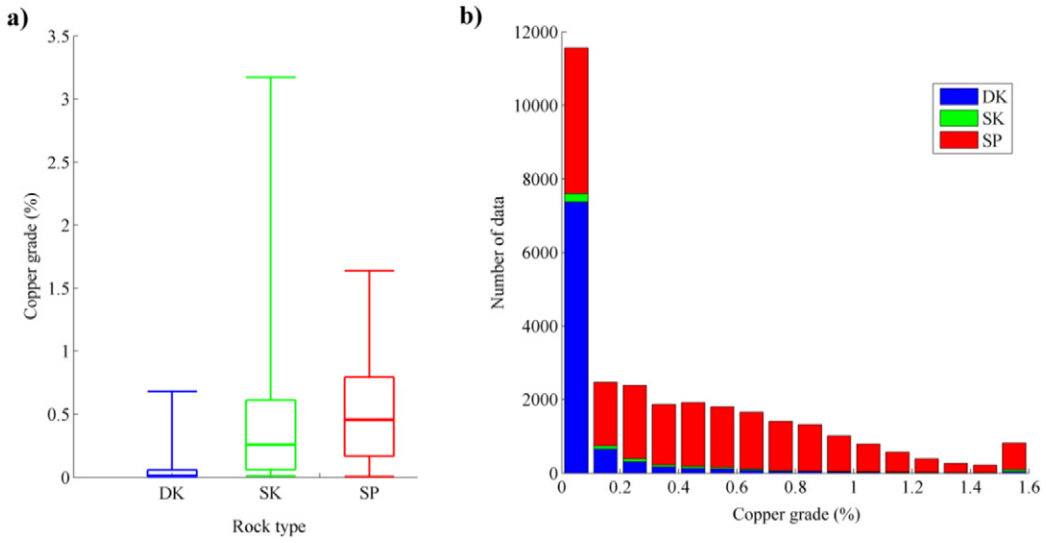

Fig. 4. a) Box plots of copper grade (drill hole data) for each rock type domain; and b) histogram of copper grades (drill hole data).

two domains. Accordingly, the rock type prevailing at a given spatial location **x** is defined in the following fashion:

- location **x** belongs to DK domain $\Leftrightarrow Y_1(\mathbf{x}) < t_1$
- location **x** belongs to SK domain $\Leftrightarrow Y_1(\mathbf{x}) \geq t_1$ and $Y_2(\mathbf{x}) < t_2$
- location **x** belongs to SP domain $\Leftrightarrow Y_1(\mathbf{x}) \geq t_1$ and $Y_2(\mathbf{x}) \geq t_2$.

The threshold values are determined in agreement with the domain proportions calculated from the drill hole data. For variogram analysis, the two Gaussian random fields Y_1 and Y_2 are assumed to be independent and their variograms are determined through their impact on the variograms of the domain indicators, which can be estimated experimentally from the drill hole data (Emery, 2007; Armstrong et al., 2011). Table 2 indicates the parameters for the variogram models obtained for the Gaussian random fields. In order to reproduce a regular boundary between late-injected dykes and the other two domains, cubic variogram models have been used for the first Gaussian random field (Y_1), since they are smooth at the origin and associated with regular boundaries (Lantuéjoul, 2002). In contrast, spherical models (linear at the origin) are used for the second Gaussian random field, which will produce a more irregular boundary between domains SK and SP, as can be observed in Fig. 1.

One hundred point-support realizations of the rock type domains are generated on a grid with a 5 m × 5 m × 2 m spacing. Fig. 5 shows a perspective view of three realizations (d, e, f), together with the probability maps (a, b, c) for the three domains calculated by dividing, at each location, the number of outcomes for a specific rock type (an integer between 0 and 100) by the number of total outcomes (100). In these maps, the red regions are associated with the locations where there is a high potential to find a specific rock type domain, while the blue regions correspond to locations where domains are quite unlikely to be present. Both red and blue regions are located around the drill holes, for which the domains have been seen directly. Finally the intermediate color regions indicate a greater uncertainty on whether or not a specific domain can be found (in particular, whether or not there is some economic mineralization). These mainly correspond to the regions in-between the drill holes and to the margins of the deposit.

3.4. Grade simulation

To assess the accuracy of the results, three different approached will be compared, as follows:

- Copper grade simulation without geological control (**A**1): in this method, sequential simulation is used to reproduce the copper grade variability, without considering a rock type partition of the deposit.
- Copper grade simulation using a deterministic geological model (**A**2): this method uses an interpreted model of the three rock type domains (SP, SK, and DK). Copper grades are then simulated independently within each domain using sequential simulation.
- Copper grade simulation using a stochastic geological model (**A**3): here, one hundred realizations of the rock type domains are obtained with plurigaussian simulation. Copper grades are then simulated independently within each simulated domain, using the cascade approach presented in Section 2.4.

In each case, the copper grades are generated using point-support simulation on the same grid as the one considered for plurigaussian simulation of the rock types (5 m × 5 m × 2 m spacing). The variograms of the Gaussian random fields that have been used for simulating the grades, inferred from the normal scores data, are indicated in Table 3.

3.5. Performance evaluation

The simulated grade models based on three approaches are validated against a model created by point-support ordinary kriging on the 5 m × 5 m × 2 m grid, given a set of 20,405 blast hole data in which

Table 2
Parameters of variogram models of underlying Gaussian random fields. Ranges and rotation angles define the ellipsoid of anisotropy for each basic structure.

Gaussian random field	Nugget	Sill	Basic structure	First range (m)	Second range (m)	Third range (m)	First angle (°)	Second angle (°)	Third angle (°)
Y_1	0.05	0.40	Cubic	200	120	80	150	0	30
		0.55	Cubic	800	600	250	150	0	30
Y_2	0	0.38	Spherical	350	250	110	150	0	0
		0.62	Spherical	1350	950	640	150	0	0

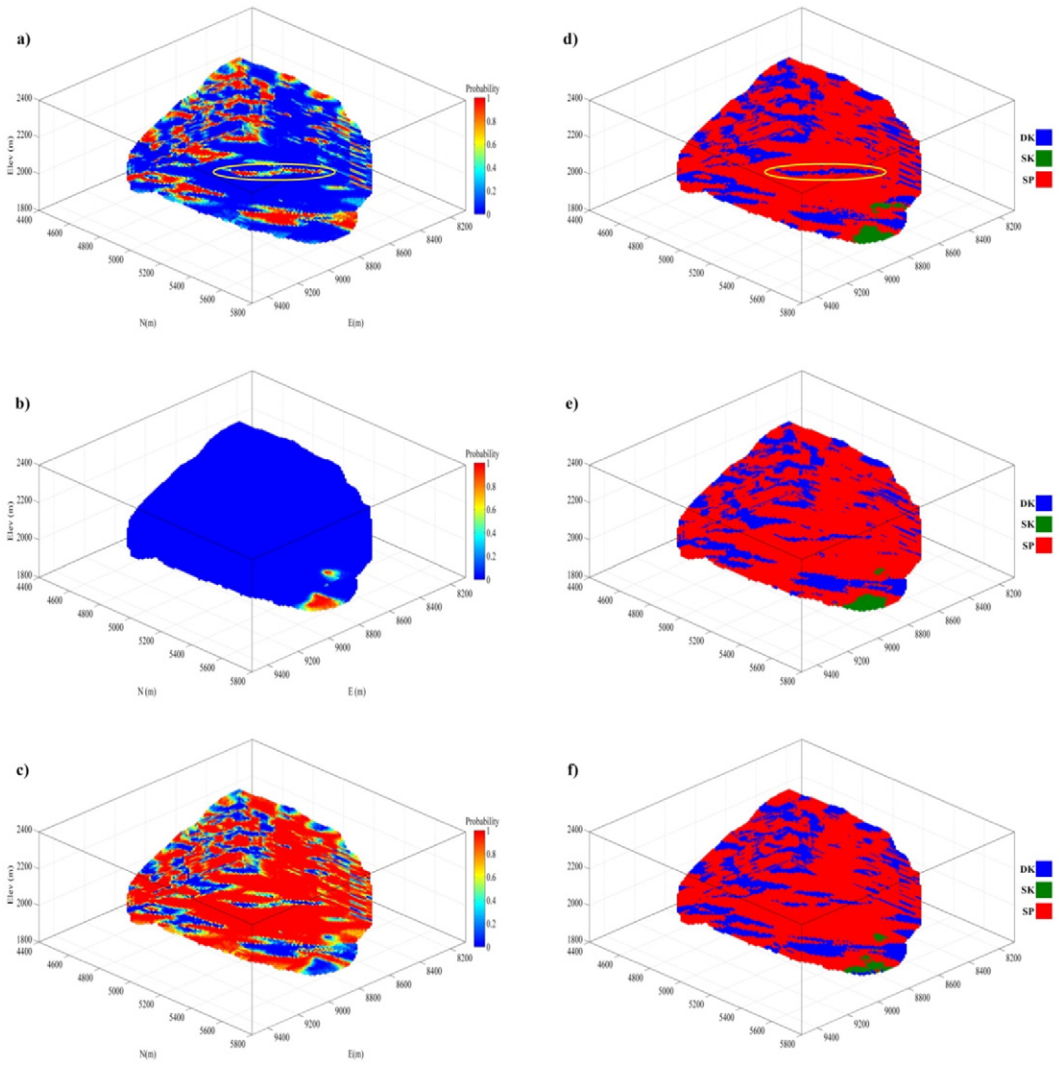

Fig. 5. Probabilities of occurrence of a) DK, b) SK, and c) SP domains, obtained from a set of 100 conditional realizations, and three conditional realizations of the rock type domains (d, e, f). Yellow ellipses in a) and d) show the probability of occurrence and a realization of a late-injected dyke, respectively, in a specific region.

the true copper grades are known. Because the mesh of blast hole data (about 5 m × 5 m × 3 m) is of the same order of magnitude as the mesh of the target grid, the kriging errors are negligible and the kriged grades are therefore considered as the true copper grades, against which the grades obtained with the different simulation approaches can be compared. In order to quantify the distribution of errors in the simulated grades, the mean error percentage (MEP) for the *k*-th realization, with $k = 1 \ldots 100$, and the linear correlation coefficient (LCC) between the *k*-th realization and the validation model are defined as follows (Cáceres and Emery, 2010):

$$MEP(k) = \frac{1}{nloc}\sum_{i=1}^{nloc} 100 \times \left(\frac{S^k(i) - R(i)}{R(i)}\right) \quad (1)$$

$$LCC(k) = \frac{nloc\sum_{i=1}^{nloc}\left(S^k(i)\,R(i)\right) - \left(\sum_{i=1}^{nloc}S^k(i)\right)\left(\sum_{i=1}^{nloc}R(i)\right)}{\sqrt{nloc\sum_{i=1}^{nloc}\left(S^k(i)\right)^2 - \left(\sum_{i=1}^{nloc}S^k(i)\right)^2}\sqrt{nloc\sum_{i=1}^{nloc}(R(i))^2 - \left(\sum_{i=1}^{nloc}R(i)\right)^2}} \quad (2)$$

where $S^k(i)$ is the simulated grade at location i, R(i) is the "real" grade obtained by kriging from the blast hole data, and *nloc* is the total number of grid locations. Fig. 6 presents the cumulative distribution functions of MEP (a) and LCC (b) calculated over the 100 realizations (one MEP value and one LCC value per realization), for each approach. Approach A3 has a MEP distribution closer to zero and an LCC distribution closer to one than the other two approaches (A1, A2) and therefore proves to be more accurate.

Table 3
Parameters of variogram models of transformed copper grades. Ranges and rotation angles define the ellipsoid of anisotropy for each basic structure.

Domain	Nugget	Sill	Basic structure	First range (m)	Second range (m)	Third range (m)	First angle (°)	Second angle (°)	Third angle (°)
Global	0.07	0.18	Spherical	165	75	60	150	0	0
SP	0.04	0.19	Spherical	170	80	60	150	0	0
SK	0.52	1.18	Spherical	170	80	40	150	0	0
DK	0.00	0.47	Spherical	270	120	40	150	0	30

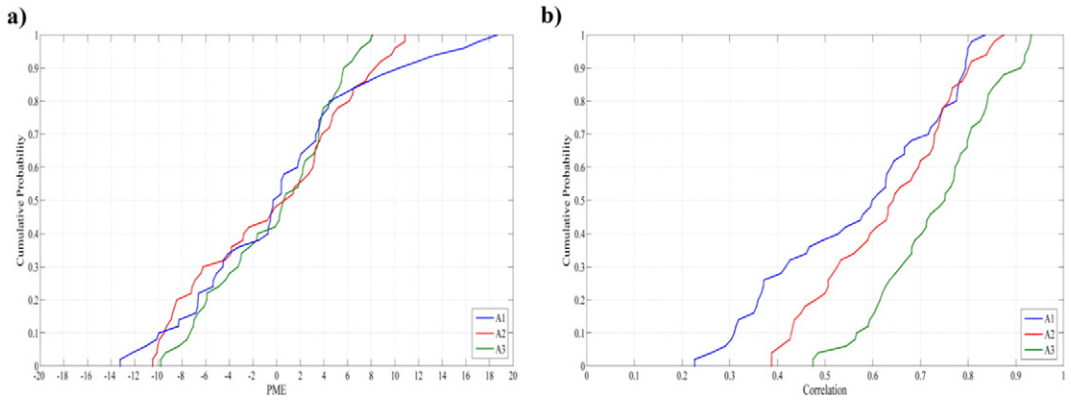

Fig. 6. Cumulative distribution functions of MEP (a) and of correlation coefficients (b) calculated over 100 realizations.

Considering that the aim of this study is to make the grade prediction more accurate, it is also of interest to avoid misclassifications between ore and waste. To this end, for each block of the grid, the selection (mill or dump) at a given cut-off based on the simulated grade is compared with the selection obtained using the "real" grade, to determine whether there is a match or not. The grand overall match percentage at the given cut-off, over all the blocks and over the 100 realizations, is then computed and plotted against the cut-off, for each approach (Fig. 7). Again, approach A3 is seen to provide consistently better results than approaches A1 and A2.

4. Discussion

As indicated in Section 3.1.3, due to the complexity in the geometry of the dykes, a deterministic model of the rock type domains is likely to misclassify the true rock type at any unsampled location. As a practical solution, this study considers a stochastic modeling of the rock types, through the use of multiple equally-probable realizations (Fig. 5), and subsequently of the copper grades, allowing modeling the joint uncertainty in rock types and grades at unsampled locations. For a better understanding the differences between each approach and how the rock type model relates to the copper grade model, compare the results in Figs. 5 and 8 simultaneously. Fig. 8a depicts the expected copper grade (calculated as the average of 100 grade realizations) without geological control (A1). From a geological point of view, the grade variation is illogical. As a representative example, the yellow ellipses in Fig. 5a and d show the probability of occurrence and a realization of a late-injected dyke, respectively. Comparing this dyke sample and the associated ellipse in Fig. 8a, it appears that the low grade of this late-injected dyke is not observed in this model. On the contrary, the second approach (A2) produces a grade model that is consistent with the structure of the DK and SP domains (Fig. 8b). According to mine geologists and to the production data, there is little variation of the copper grade in the DK domain. However, this approach has some limitations; in particular the obtained grade model is strongly dependent on the interpretation of the geologist about the boundaries of the rock type domains. As a result, one obtains a grade model with clear-cut discontinuities when passing from one domain to another (Fig. 8b), but the position of such discontinuities may be mistaken due to geological interpretation errors, in particular, in relation to the complicated structure of the late-injected dykes. In contrast, in the cascade simulation approach (A3), the uncertainty in the layout of the rock type domains is considered through the construction of 100 different realizations of the geological domains. Although the discontinuities still exist in each individual realization of the copper grade, the expected copper grade (calculated by averaging the 100 grade realizations) no longer exhibits such discontinuities (Fig. 8c), which is explained because one does not exactly know the position of domain boundaries: a given location classified as dyke in some realizations and simulated with a very low copper grade, may be classified as ore (SK or SP) and simulated with a higher copper grade in other realizations, resulting in an intermediate average grade over the realizations and no clear-cut discontinuities between ore and waste in this average model.

In addition to averaging the copper grade realizations, one can calculate the variance of the grade realizations at each target location (Fig. 8d, e, f), which measures the uncertainty in the true unknown grades. A strong dependence between the variance and the expected grades is evident in each approach. The explanation of this observation stems from a property of the spatial grade distribution known as proportional effect, according to which high-grade areas have a greater variability than low-grade areas. However, the grade models based on a deterministic (A2) or probabilistic (A3) modeling of the rock type domains show significantly lower variances than the grade model obtained without geological control (A1), suggesting that the incorporation of the rock type information reduces the uncertainty in the grade models.

Because it relies on a single rock type model, approach A2 is likely to misclassify the rock type domains when the geology gets complex. The errors in the rock type model affect the predicted grades and tonnages of ore, and eventually all the future mining plans. For instance, in approach A2, for a zero cut-off grade (i.e., without any selection on the copper grade), the tonnage of ore rocks (SK and SP, excepting DK considered as waste) is equal to 1158 million tonnes in all the realizations (Fig. 9a). This method uses just one layout of the rock type domains and there is no measurement for uncertainty in such a layout, while for a cut-off grade of 0.3%, the tonnage of ore rocks fluctuates between 598.5 and 667.1 million tonnes, depending on the realization, with an average of 631.7 million tonnes (Fig. 9b). In contrast, for the same cut-off grades, approach A3 yields a larger range for the tonnage of SK and

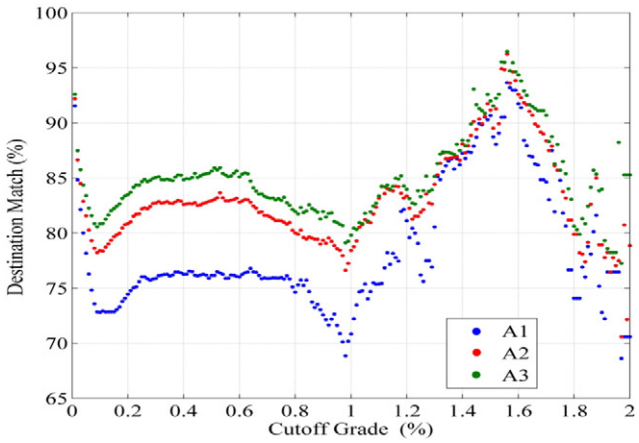

Fig. 7. Percentage of correct classification.

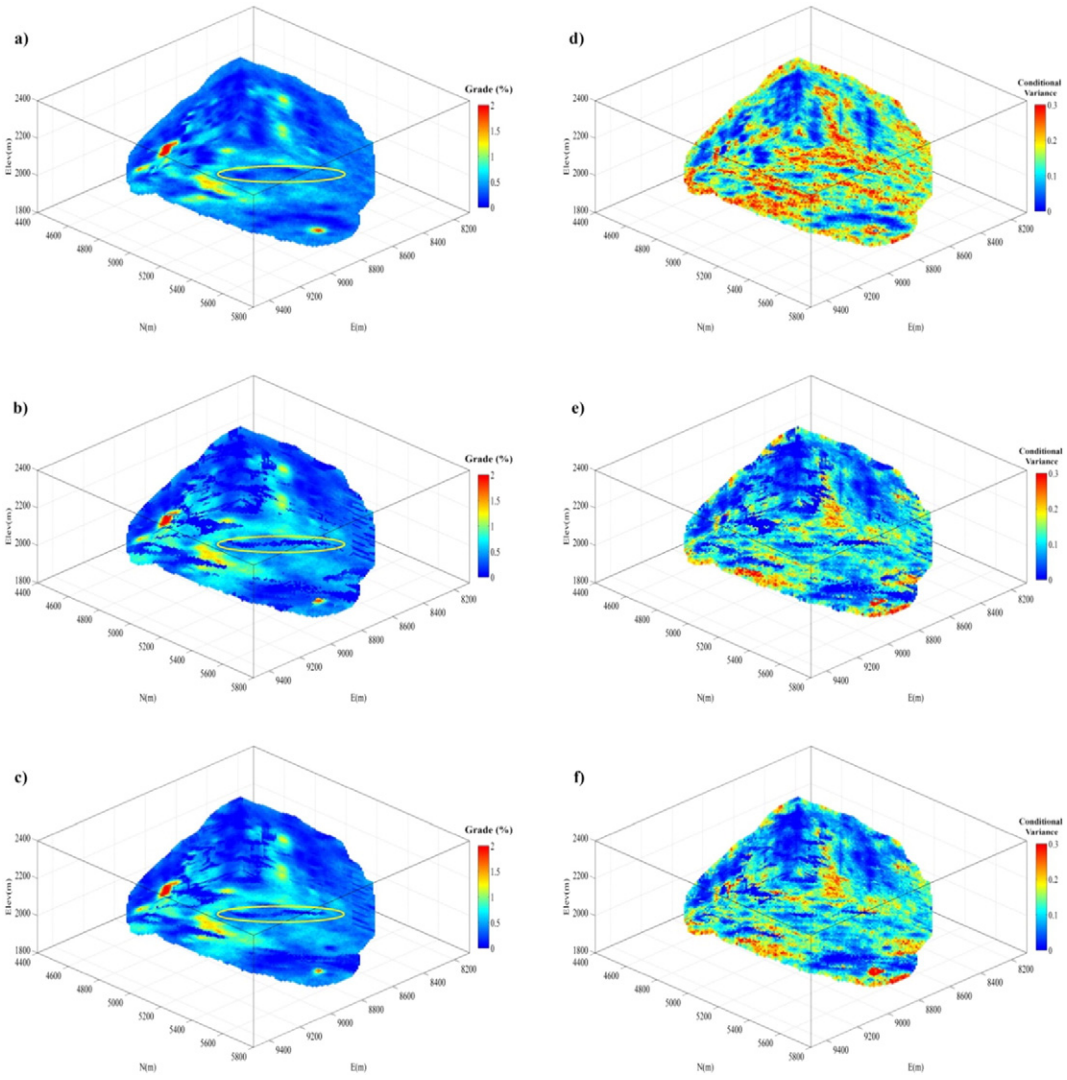

Fig. 8. Mean (a, b, c) and variance (d, e, f) of the simulated copper grades using approaches A1, A2 and A3, respectively (calculations from 100 realizations). Yellow ellipses in a), b), and c) show the expected copper grade for the late-injected dyke located as in the geological model in Fig. 5.

SP (between 1146.8 and 1212.0 million tonnes at cut-off 0%, and between 598.2 and 696.1 million tonnes at cut-off 0.3%), which is explained because the layouts of both domains SK and SP vary from one realization to another, causing greater uncertainty in their tonnages. Approach A1 does not provide such information, as no lithological model is available in this approach (only a grade model).

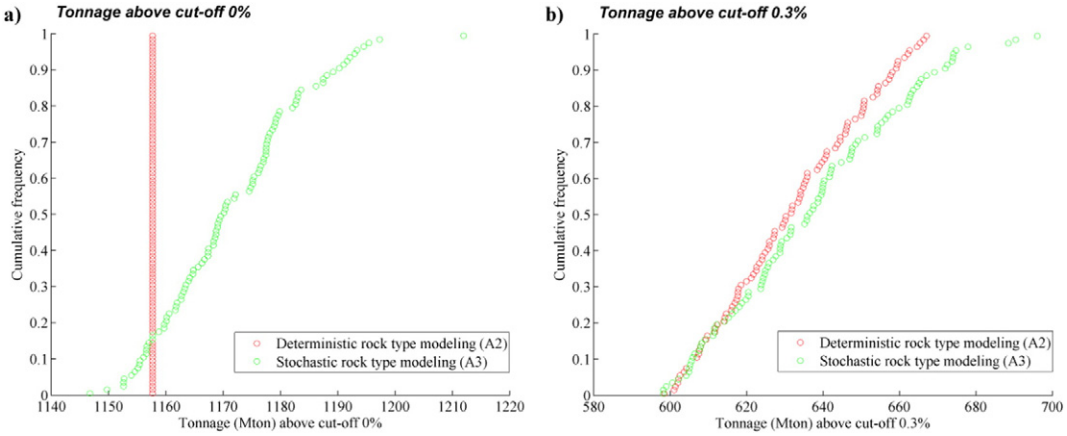

Fig. 9. Distribution of the tonnage of ore material above cut-off 0% (a) and above cut-off 0.3% (b), calculated over 100 realizations of approaches A2 (red) and A3 (green).

5. Conclusions

In the Sungun porphyry copper deposit, the dyke domain has no economic mineralization and should not be considered in the mineral resource evaluation step, while the porphyry and skarn domains have different copper grade distributions and should be separated from each other in the resource evaluation stage. Dykes have a very complicated structure and make a big challenge for the mine geologists to interpret their layout. A deterministic interpretation is logically unable to reproduce the true spatial variability and to measure the uncertainty in the domain layouts, which may produce a significant error in the resulting copper grade models. As an alternative to this approach, this study focused on a probabilistic simulation of the geological domains, using the plurigaussian model, and afterward combining the rock type simulation with a copper grade simulation within each rock type. The proposed approach improves the accuracy of the expected grades when validating the realizations against production data. Stochastic mine planning approaches should therefore consider the influence of probabilistic rock type modeling to grade evaluation in order to allow better decision-making for mine executives.

Acknowledgments

This research was supported by the National Iranian Copper Industry Company (NICICo) and by CONICYT PIA Anillo ACT 1407. The authors are also grateful to Sungun copper mine for providing the data set used in this work.

References

Afshooni, S.Z., Mirnejad, H., Esmaeily, D., Asadi Haroni, H., 2013. Mineral chemistry of hydrothermal biotite from the Kahang porphyry copper deposit (NE Isfahan), Central Province of Iran. Ore Geol. Rev. 54, 214–232.

Armstrong, M., Galli, A., Beucher, H., Le Loc'h, G., Renard, D., Doligez, B., Eschard, R., Geffroy, F., 2011. Plurigaussian Simulations in Geosciences. second ed. Springer, Berlin (176 pp.).

Asghari, O., Hezarkhani, A., Soltani, F., 2009. The comparison of alteration zones in the Sungun porphyry copper deposit, Iran (based on fluid inclusion studies). Acta Geol. Pol. 59, 93–109.

Azadi, M., Mirmohammadi, M., Hezarkhani, A., 2015. Aspects of magmatic–hydrothermal evolution of Kahang porphyry copper deposit, Central Iran. Arab. J. Geosci. 8, 4873–4893.

Boomeri, M., Nakashima, K., Lentz, D.R., 2010. The Sarcheshmeh porphyry copper deposit, Kerman, Iran: a mineralogical analysis of the igneous rocks and alteration zones including halogen element systematics related to Cu mineralization processes. Ore Geol. Rev. 38, 367–381.

Cáceres, A., Emery, X., 2010. Conditional Co-simulation of Copper Grades and Lithofacies in the Rio Blanco-Los Bronces Copper Deposit. In: Castro, R., Emery, X., Kuyvenhoven, R. (Eds.), Proceedings of the IV International Conference on Mining Innovation MININ 2010. Gecamin Ltd, Santiago, Chile, pp. 311–320.

Calagari, A.A., 2003. Stable isotope (S, O, H and C) studies of phyllic and potassic–phyllic alteration zones of the porphyry copper deposit at Sungun, East Azarbaidjan, Iran. J. Asian Earth Sci. 21, 767–780.

Calagari, A.A., 2004. Geology and fracture-related hypogene hydrothermal alteration and mineralization of porphyry copper deposit at Sungun. J. Geol. Soc. India 64 (5), 595–618.

Calagari, A.A., Hosseinzadeh, G., 2006. The mineralogy of copper-bearing skarn to the east of the Sungun-Chay river, East-Azarbaidjan, Iran. J. Asian Earth Sci. 28, 423–438.

Chilès, J.P., Delfiner, P., 2012. Geostatistics: Modeling Spatial Uncertainty. second ed. Wiley, New York.

Dargahi, S., Arvin, M., Pan, Y., Babaei, A., 2010. Petrogenesis of post-collisional A-type granitoids from the Urumieh–Dokhtar magmatic assemblage, Southwestern Kerman, Iran: constraints on the Arabian–Eurasian continental collision. Lithos 115, 190–204.

Deutsch, C.V., 2006. A sequential indicator simulation program for categorical variables with point and block data: BlockSIS. Comput. Geosci. 32, 1669–1681.

Deutsch, C.V., Journel, A.G., 1998. GSLIB: Geostatistical Software Library and User's Guide. Oxford University Press, New York.

Dowd, P.A., 1986. Geometrical and geological controls in geostatistical estimation and ore body modelling. In: Ramani, R.V. (Ed.), Proceedings of the 19th APCOM Symposium. Society of Mining Engineers, Littleton, Colorado, pp. 81–99.

Duke, J.H., Hanna, P.J., 2001. Geological interpretation for resource modelling and estimation. In: Edwards, A.C. (Ed.), Mineral Resource and Ore Reserve Estimation—The AusIMM Guide to Good Practice. The Australasian Institute of Mining and Metallurgy, Melbourne, pp. 147–156.

Emery, X., 2007. Simulation of geological domains using the plurigaussian model: new developments and computer programs. Comput. Geosci. 33 (9), 1189–1201.

Etminan, H., 1977. The Discovery of Porphyry Copper–Molybdenum Mineralization Adjacent to Sungun Village in the Northwest of Ahar and a Proposed Program for its Detailed Exploration. Geological Report. Geological Survey of Iran (26 pp.).

Galli, A., Beucher, H., Le Loc'h, G., Doligez, B., Group, H., 1994. The Pros and Cons of the Truncated Gaussian Method. In: Armstrong, M., Dowd, P.A. (Eds.), Geostatistical Simulations. Kluwer Academic, Dordrecht, pp. 217–233.

Goovaerts, P., 1997. Geostatistics for Natural Resources Evaluation. Oxford University Press, New York (496 pp.).

Hezarkhani, A., 2002. Specific physico-chemical conditions (360 °C) for chalcopyrite dissolution/deposition in the Sungun Porphyry Copper Deposit, Iran. Amirkabir J. Sci. Technol. 13 (52), 668–687.

Hezarkhani, A., 2006a. Petrology of intrusive rocks within the Sungun porphyry copper deposit, Azarbaijan, Iran. J. Asian Earth Sci. 27 (3), 326–340.

Hezarkhani, A., 2006b. Hydrothermal evolution of the Sarcheshmeh porphyry Cu–Mo deposit, Iran: evidence from fluid inclusions. J. Asian Earth Sci. 28, 409–422.

Hezarkhani, A., Williams-Jones, A.E., 1998. Controls of alteration and mineralization in the Sungun porphyry copper deposit, Iran: evidence from fluid inclusions and stable isotopes. Econ. Geol. 93, 651–670.

Hou, Z., Zhang, H., Pan, X., Yang, Z., 2011. Porphyry Cu (−Mo–Au) deposits related to melting of thickened mafic lower crust: examples from the eastern Tethyan metallogenic domain. Ore Geol. Rev. 39, 21–45.

Journel, A.G., Alabert, F., 1990. New method for reservoir mapping. J. Pet. Technol. 42 (2), 212–218.

Journel, A.G., Gómez-Hernández, J.J., 1993. Stochastic imaging of the Wilmington clastic sequence. SPE Form. Eval. 8 (1), 33–40.

Lantuéjoul, C., 2002. Geostatistical Simulation: Models and Algorithms. Springer, Berlin.

Le Loc'h, G., Beucher, H., Galli, A., Doligez, B., Group, H., 1994. Improvement in the Truncated Gaussian Method: Combining Several Gaussian Functions. Proceedings ECMOR IV, 4th European Conference on the Mathematics of Oil Recovery, Røros, Norway (13 pp.).

Lescuyer, J.L., Riou, R., Babakhani, A., Alavi Tehrani, N., Nogol, M.A., Dido, J., Gemain, Y.M., 1978. Geological Map of the Ahar Area. Geological Survey of Iran.

Madani, N., Emery, X., 2015. Simulation of geo-domains accounting for chronology and contact relationships: application to the Río Blanco copper deposit. Stoch. Env. Res. Risk A. http://dx.doi.org/10.1007/s00477-014-0997-x.

Mariethoz, G., Caers, J., 2015. Multiple-point Geostatistics: Stochastic Modeling With Training Images. John Wiley & Sons, Ltd.

Matheron, G., Beucher, H., Galli, A., Guérillot, D., Ravenne, C., 1987. Conditional simulation of the geometry of fluvio-deltaic reservoirs. 62nd Annual Technical Conference and Exhibition of the Society of Petroleum Engineers. SPE Paper 16753, Dallas, pp. 591–599.

Mehrpartou, M., 1993. Contributions to the geology, geochemistry, ore genesis and fluid inclusion investigations on Sungun Cu–Mo porphyry deposit, Northwest of Iran. Unpublished PhD Thesis. University of Hamburg, Germany, 245 pp.

Remy, N., Boucher, A., Wu, J., 2009. Applied Geostatistics With SGeMS: A User's Guide. Cambridge University Press, Cambridge (284 pp.).

Rezaee, H., Asghari, O., Koneshloo, M., Ortiz, J.M., 2014. Multiple-point geostatistical simulation of dykes: application at Sungun porphyry copper system, Iran. Stoch. Env. Res. Risk A. 28 (7), 1913–1927.

Riquelme, R., Le Loc'h, G., Carrasco, P., 2008. Truncated Gaussian and Plurigaussian Simulations of Lithological Units in Mansa Mina Deposit. In: Ortiz, J.M., Emery, X. (Eds.), Proceedings of the 8th International Geostatistics Congress. Gecamin Ltda, Santiago, Chile, pp. 819–828.

Roldão, D., Ribeiro, D., Cunha, E., Noronha, R., Madsen, A., Masetti, L., 2012. Combined Use of Lithological and Grade Simulations for Risk Analysis in Iron Ore, Brazil. In: Abrahamsen, P., Hauge, R., Kolbjørnsen, O. (Eds.), Geostatistics Oslo. Springer, Berlin, pp. 423–434.

Rossi, M.E., Deutsch, C.V., 2014. Mineral Resource Estimation. Springer, Dordrecht.

Shafiei, B., 2010. Lead isotope signatures of the igneous rocks and porphyry copper deposits from the Kerman Cenozoic magmatic arc (SE Iran), and their magmatic–metallogenetic implications. Ore Geol. Rev. 38, 27–36.

Shahabpour, J., 2005. Tectonic evolution of the orogenic arc in the region located between Kerman and Neyriz. J. Asian Earth Sci. 24, 405–417.

Shahabpour, J., 2007. Island-arc affinity of the Central Iranian Volcanic Belt. J. Asian Earth Sci. 30, 652–665.

Sinclair, A.J., Blackwell, G.H., 2002. Applied Mineral Inventory Estimation. Cambridge University Press, Cambridge (381 pp.).

Strebelle, S., 2002. Conditional simulation of complex geological structures using multiple-point statistics. Math. Geol. 34 (1), 1–22.

Talebi, H., Asghari, O., Emery, X., 2013. Application of plurigaussian simulation to delineate the layout of alteration domains in Sungun copper deposit. Cent. Eur. J. Geosci. 5 (4), 514–522.

Talebi, H., Asghari, O., Emery, X., 2014. Simulation of the late-injected dykes in an Iranian porphyry copper deposit using the plurigaussian model. Arab. J. Geosci. 7 (7), 2771–2780.

Yunsel, T.Y., Ersoy, A., 2013. Geological modeling of rock type domains in the Balya (Turkey) lead–zinc deposit using plurigaussian simulation. Cent. Eur. J. Geosci. 5 (1), 78–89.